Microscopic Gain Modeling of Semiconductor Lasers Considering Higher-Order Many-Body Effects

Hideaki Tsuchiya, Kosuke Komaki, and Tanroku Miyoshi

Department of Electrical and Electronics Engineering
Kobe University, 1-1, Rokko-dai, Nada-ku, Kobe 657-8501, Japan
Phone & Fax: +81-78-803-1073
E-mail: tsuchiya@eedept.kobe-u.ac.jp

1. Introduction

The intraband relaxation process is one of the most important mechanisms in basic optical properties of semiconductor lasers. By interacting with other particles such as phonons, photons and plasmons, a phase of electron dipole is destroyed, which results in spectral broadening in the emitted lightwave. So far, such a spectral broadening effect has often been taken into account by using a Lorentzian function with a phenomenological relaxation time approximation in the density matrix theory [1]. However, it was pointed out that the optical gain spectra calculated with the Lorentzian function deviate from the experimental data, especially, an anomalous absorption region appears at photon energies below the band-gap [2]-[5]. Then, Yamanishi and Lee [2] and Asada [3] have assumed that the intraband relaxation process is not Markovian, and derived the non-Markovian spectral broadening function from the microscopic Hamiltonians. Then, they have replaced the Lorentzian broadening function in the usual density matrix theory by it. However, this replacement has not been proved to be correct yet [4]. As an alternative non-Markovian theory of intraband relaxation, Tomita and Suzuki [4] and Ahn [5] derived a new density matrix equation from the microscopic interaction Hamiltonian including carrier scattering terms. In their theory, the intraband relaxation effect is expressed by Hamiltonian autocorrelation functions. However, unfortunately, since they approximated the Hamiltonian autocorrelation function by the simple Gaussian function with a constant correlation time, the gain spectra greatly depend on the uncertain correlation time in the actual evaluation.

In this paper, we study a microscopic derivation of spectral broadening function in semiconductor lasers based upon the nonequilibrium Green's function technique [6,7]. In this approach, various scattering phenomena such as electron-electron, electron-phonon, electron-impurity interactions are incorporated in terms of self-energy functions. In semiconductor lasers, the carrier-carrier (C-C) scattering and the LO-phonon scattering are considered as dominant carrier relaxation effects. In particular, the influence of the higher-order many-body effects, which are called as first vertex corrections, is investigated in detail.

2. Quantum Kinetic Theory of Semiconductor Laser

Dyson Equations

To understand the carrier-photon dynamics in the semiconductor gain materials, we have to consider the fact that the electron-hole plasma properties are strongly influenced by the many-body Coulomb effects, the coupling to light field, and the interaction with crystal lattice. By using the standard functional derivative technique [8], the following Dyson equations of carriers, photons and plasmons are derived.

$$\sum_{c=a,b}\int d\underline{2}\,[G^{-1}_{0,ac}(\underline{1},\underline{2}) - \Sigma_{ac}(\underline{1},\underline{2})]G_{cb}(\underline{2},\underline{1}') = \delta_{ab}\delta(\underline{1}-\underline{1}'), \quad (1)$$

$$\int d\underline{2}\,[D_0^{-1}(\underline{1},\underline{2}) - P(\underline{1},\underline{2})]D(\underline{2},\underline{1}') = \delta(\underline{1}-\underline{1}'), \quad (2)$$

$$\int d\underline{2}\,[V_0^{-1}(\underline{1},\underline{2}) - p(\underline{1},\underline{2})]V_s(\underline{2},\underline{1}') = \delta(\underline{1}-\underline{1}'), \quad (3)$$

where the compact notation of space time arguments $\underline{1} = \{\boldsymbol{r}_1, \underline{t}_1\}$ is used and the underlined time arguments are defined on the generalized Keldysh time contour [8]. $G(\Sigma)$, $D(P)$ and $V_s(p)$ are the Green's functions (the self-energies) for carriers, photons and plasmons, respectively, where $a, b = e(\text{electron}), h(\text{hole})$. In addition, the subscript "0" denotes the free Green's function describing the motion of the noninteracting particles. However, G_0 for noninteracting carriers are defined under the influence of the averaged Hartree and vector potential. The phonon's Dyson equation is omitted because the phonon system is assumed to be in equilibrium.

All interaction processes are included in the self energy functions, which can be approximated in a systematic way by using the functional derivative technique. Introducing the first vertex approximation in the infinite

0-7803-4369-7/98 $10.00 ©1998 IEEE

hierarchy of the self energy functions [6], we obtain

$$\Sigma^D_{aa}(\underline{1},\underline{2}) = i\hbar\mu_0|j_{a\bar{a}}|^2[G_{\bar{a}\bar{a}}(\underline{1},\underline{2})D(\underline{2},\underline{1}) + i\hbar e^2\int d\underline{3}d\underline{4} \times G_{\bar{a}\bar{a}}(\underline{1},\underline{3})G_{\bar{a}\bar{a}}(\underline{3},\underline{4})G_{aa}(\underline{4},\underline{2})D(\underline{4},\underline{1})V_s(\underline{2},\underline{3})], \quad (4)$$

$$\Sigma^V_{aa}(\underline{1},\underline{2}) = i\hbar e^2[G_{aa}(\underline{1},\underline{2})V_s(\underline{2},\underline{1}) + i\hbar e^2\int d\underline{3}d\underline{4} \times G_{aa}(\underline{1},\underline{3})G_{aa}(\underline{3},\underline{4})G_{aa}(\underline{4},\underline{2})V_s(\underline{4},\underline{1})V_s(\underline{2},\underline{3})], \quad (5)$$

for the photon (D) and plasmon (V) contribution to the carrier self-energy Σ, where $j_{a\bar{a}}$ denotes the interband current density matrix element. $\bar{a}$ means hole when a indicates electron, and vice versa. Similarly, the photon self-energy, $P = P_{eh} + P_{he}$, is given by

$$P_{a\bar{a}}(\underline{1},\underline{2}) = -i\hbar\mu_0|j_{a\bar{a}}|^2[G_{\bar{a}\bar{a}}(\underline{1},\underline{2})G_{aa}(\underline{2},\underline{1}) + i\hbar e^2\int d\underline{3}d\underline{4} \times G_{\bar{a}\bar{a}}(\underline{1},\underline{3})G_{\bar{a}\bar{a}}(\underline{3},\underline{2})G_{aa}(\underline{2},\underline{4})G_{aa}(\underline{4},\underline{1})V_s(\underline{4},\underline{3})]. \quad (6)$$

Here, the first term of these equations is called as the random phase approximation (RPA) contribution, while the second term the first vertex correction through the Coulomb interaction. The RPA includes the exchange energy and the partial correlation energy, while the first vertex terms represent the higher-order correlation energies neglected in RPA [9]. Here note that the plasmon Green's function V_s governed by its own equation of motion (3) is approximated by the screened Coulomb potential by introducing the quasistatic plasmon pole approximation [6], where the plasmon self-energy, $p = p_{ee} + p_{hh}$, is represented within RPA as

$$p_{aa}(\underline{1},\underline{2}) \simeq -i\hbar e^2 G_{aa}(\underline{1},\underline{2})G_{aa}(\underline{2},\underline{1}). \quad (7)$$

Further, the phonon contribution (d) to the carrier self-energy is also approximated within RPA as

$$\Sigma^d_{aa}(\underline{1},\underline{2}) \simeq i\hbar e^2 G_{aa}(\underline{1},\underline{2})d(\underline{2},\underline{1}), \quad (8)$$

where d is the phonon Green's function in equilibrium [7].

Optical Gain

In this paper, since we focus on the gain properties before lasing, the photon contribution to the carrier self-energy will be neglected, and then $\Sigma \simeq \Sigma^V + \Sigma^d$. The optical gain is given by the imaginary part of the retarded photon self-energy. After decomposing the matrix photon self-energy according to ref. 8 on the Keldysh contour and then Fourier transforming the retarded self-energy with respect to $(\boldsymbol{r}_1 - \boldsymbol{r}_2, t_1 - t_2)$, we obtain the following optical gain rate.

$$g(\Omega) = \frac{2\pi e^2}{nm_0^2\varepsilon c\Omega}|M|^2\int\frac{d^3\mathbf{k}}{(2\pi)^3}L_{eh}(\mathbf{k},\Omega)w(\mathbf{k},\Omega) \times [f_e(\mathbf{k}) + f_h(\mathbf{k}) - 1], \quad (9)$$

where $w(\mathbf{k},\Omega)$ is the Coulomb enhancement function expressed by

$$w(\mathbf{k},\Omega) = 1 + \hbar e^2\int\frac{d^3\mathbf{k}'}{(2\pi)^3}\int\frac{d\omega'}{2\pi}V_s^r(\mathbf{k}-\mathbf{k}')\Big\{\hat{A}_{ee}(\mathbf{k}',\omega') \times \mathrm{Re}\,[G^r_{hh}(\mathbf{k}',\omega'-\Omega)]\,[1-2f_e(\mathbf{k}')] - \mathrm{Re}\,[G^r_{ee}(\mathbf{k}',\omega')]\,\hat{A}_{hh}(\mathbf{k}',\omega'-\Omega)\,[1-2f_h(\mathbf{k}')]\Big\}, \quad (10)$$

where the second term represented in the integral form denotes the first vertex corrections, which leads to the Coulomb enhancement effects in the laser gain spectra. Here ω and Ω indicate the frequency of carriers and photons, respectively. $L_{eh}(\mathbf{k},\Omega)$ is the photon spectral shape function defined by

$$L_{eh}(\mathbf{k},\Omega) = \int\frac{\hbar d\omega}{(2\pi)^2}\hat{A}_{ee}(\mathbf{k},\omega)\hat{A}_{hh}(\mathbf{k},\omega-\Omega). \quad (11)$$

In the derivations of these equations, we have used the relation $|j_{a\bar{a}}|^2 = (e^2/2m_0^2)|M|^2$ with the momentum transition matrix element M, and a carrier quasiparticle approximation (Kadanoff-Baym approximation) given by

$$G^<_{ee}(\mathbf{k},\omega) = i\hat{A}_{ee}(\mathbf{k},\omega)f_e(\mathbf{k}), \quad (12)$$

where $\hat{A}_{aa}(\mathbf{k},\omega)$ is the intraband carrier spectral function and $f_a(\mathbf{k})$ is the carrier distribution function. The intraband spectral function is generally defined as the imaginary part of the retarded Green's function as

$$\hat{A}_{aa}(\mathbf{k},\omega) = -2\mathrm{Im}\frac{1}{\omega - \omega^a_{\mathbf{k}} - \Sigma^r_{aa}(\mathbf{k},\omega)}, \quad (13)$$

where $\omega^a_{\mathbf{k}}$ denotes the free carrier's frequency. The carrier spectral function (13) represents the energy-momentum dispersion relation of interacting carriers. For noninteracting carriers, eq. (13) is simply written by $\hat{A}_{aa}(\mathbf{k},\omega) = 2\pi\delta(\omega - \omega^a_{\mathbf{k}})$.

Carrier Retarded Self-Energy

In this section, we present the carrier retarded self-energies to evaluate the photon spectral function. First, the self-energy due to the C-C scattering is derived as

$$[\Sigma^V_{aa}(\mathbf{k},\omega)]^r = \frac{\hbar^2 e^4}{(2\pi)^6}\int d^3\mathbf{k}_1 d^3\mathbf{k}_2 \times \Bigg[\frac{|V^r_s(\mathbf{k}_1-\mathbf{k})|^2}{\hbar\omega - \epsilon^a_{\mathbf{k}_1} - \epsilon^a_{\mathbf{k}_2} + \epsilon^a_{\mathbf{k}_2+\mathbf{k}_1-\mathbf{k}} + i\eta}F^a_1 + \frac{|V^r_s(\mathbf{k}_1-\mathbf{k})|^2}{\hbar\omega - \epsilon^a_{\mathbf{k}_1} - \epsilon^{\bar{a}}_{\mathbf{k}_2} + \epsilon^{\bar{a}}_{\mathbf{k}_2+\mathbf{k}_1-\mathbf{k}} + i\eta}F^a_2 - \frac{V^r_s(\mathbf{k}_1-\mathbf{k})V^r_s(\mathbf{k}_2-\mathbf{k})}{\hbar\omega - \epsilon^a_{\mathbf{k}_1} - \epsilon^a_{\mathbf{k}_2} + \epsilon^a_{\mathbf{k}_2+\mathbf{k}_1-\mathbf{k}} + i\eta}F^a_1\Bigg], \quad (14)$$

where η is infinitesimal and

$$F^a_1 = [1-f_a(\mathbf{k}_1)]f_a(\mathbf{k}_2+\mathbf{k}_1-\mathbf{k})[1-f_a(\mathbf{k}_2)] + f_a(\mathbf{k}_1)[1-f_a(\mathbf{k}_2+\mathbf{k}_1-\mathbf{k})]f_a(\mathbf{k}_2), \quad (15)$$

$$F^a_2 = [1-f_a(\mathbf{k}_1)][1-f_{\bar{a}}(\mathbf{k}_2+\mathbf{k}_1-\mathbf{k})]f_{\bar{a}}(\mathbf{k}_2) + f_a(\mathbf{k}_1)f_{\bar{a}}(\mathbf{k}_2+\mathbf{k}_1-\mathbf{k})[1-f_{\bar{a}}(\mathbf{k}_2)]. \quad (16)$$

Here, the first and second terms on the right-hand side of eq. (14) denote the intraband and interband Coulomb interactions within RPA, respectively, and the third line the first vertex corrections. It should be noticed that the first vertex corrections probably cancel out the RPA contributions, because their signs are opposite. Next, the self-energy due to the LO-phonon scattering is derived by using the screened phonon Green's function as

$$[\Sigma^d_{aa}(\mathbf{k},\omega)]^r = \frac{e^2\omega_{LO}}{2}\left(\frac{1}{\varepsilon_\infty}-\frac{1}{\varepsilon_0}\right)\int\frac{d^3\mathbf{k}'}{(2\pi)^3}\frac{|\mathbf{k}-\mathbf{k}'|^2}{[|\mathbf{k}-\mathbf{k}'|^2+\kappa^2]^2} \times\left[\frac{N_{LO}+1-f_e(\omega^e_{\mathbf{k}'})}{\omega-\omega_{LO}-\omega^e_{\mathbf{k}'}+i\eta}+\frac{N_{LO}+f_e(\omega^e_{\mathbf{k}'})}{\omega+\omega_{LO}-\omega^e_{\mathbf{k}'}+i\eta}\right], \quad (17)$$

where the LO-phonon number and frequency are assumed to be constant and given by N_{LO} and ω_{LO}, respectively, and κ is the screening wavenumber. Here, we emphasize that the energy dependence of the carrier self-energies is exactly included in eqs. (14) and (17).

3. Simulated Results

In all calculations, the lattice-temperature is 300K and the carrier density $3 \times 10^{18}\text{cm}^{-3}$. Fig. 1 shows the photon spectral shape functions at band edge ($k = 0$) computed for bulk GaAs semiconductor lasers, where the C-C scattering and the LO-phonon scattering contributions are plotted separately in (a) and (b), respectively. For reference, the result within the RPA is also plotted in Fig. 1 (a). First, since the first vertex corrections cancel out the RPA contributions, the broadening function is modified to be narrower than that of RPA as shown in Fig. 1 (a). In addition, the shape function is slightly asymmetric across the band-gap $E_g = 1.424$eV. Next, Fig.1 (b) reveals a rather complicated and asymmetric shape function with the phonon side-band peaks at the energies $E_g \pm \hbar\omega_{LO}$. By combining the results of Fig. 1 (a) and (b), the total photon spectral shape function is obtained as shown in Fig. 2, where the curves within the RPA in the C-C scattering and the Lorentzian function ($\tau_{in} = 0.1$ps) are also plotted. The phonon side-band peaks are still observed in the solid and the dashed lines. Here, note that at the energy region below the band-gap, the Lorentzian function converges quite slowly, which leads to an anomalous absorption below the band-gap.

Fig. 3 shows the computed energy-momentum diagram of the photon spectral shape function. The dark region follows the parabolic dispersion curve given by the reduced effective mass of electrons and holes, and the extent of broadening is represented by shading. It is found that the spectral broadening depends on the carrier wavenumber so that the broadening becomes narrower as the wavenumber increases. This is due to the fact that the higher velocity carriers are less scattered compared with the lower velocity carriers. By using the data of Fig. 3, the optical gain spectra are evaluated as shown in Fig. 4. First, the peak gain is increased from that of RPA by including the first vertex correction in the C-C scattering. Next, the interband Coulomb enhancement (CE) effects, which comes from the first vertex contributions

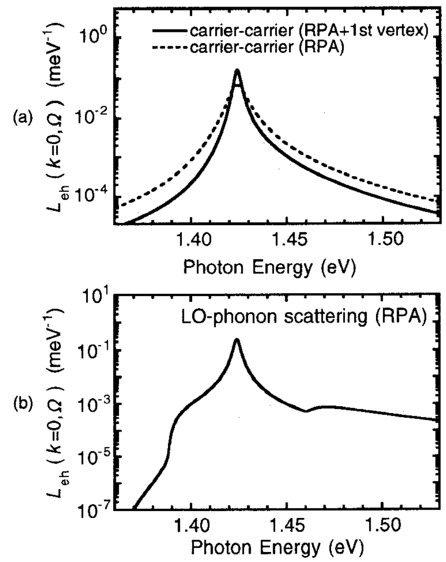

Figure 1: Photon spectral shape functions at band edge (k=0) with (a) carrier-carrier scattering and (b) carrier-LO phonon scattering.

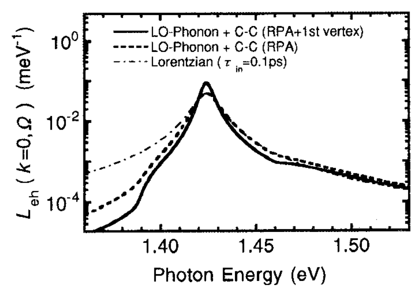

Figure 2: Total photon spectral shape function at k=0.

in eq. (10), causes the peak gain to further increase, because the interband Coulomb attraction of electrons and holes leads to the enhancement of the optical transition probabilities. The above results mean that the first vertex corrections significantly influence the gain properties of semiconductor lasers operating in the high density regime. Here, we notice that the gain curve estimated by the Lorentzian function exhibits an unreasonable negative gain region below the band-gap.

Finally, our results are compared with the quasiparticle energy approximation [6], where the energy dependence of the carrier self-energy $\Sigma^r_{aa}(\mathbf{k},\omega)$ is approximated as $\Sigma^r_{aa}(\mathbf{k})$ by using the quasiparticle relation of $\omega = \omega^a_{\mathbf{k}}(= \hbar\mathbf{k}^2/2m_a)$. Fig. 5 shows the comparison between our result and the quasiparticle energy approximation for (a) the photon spectral shape functions at $k = 0$ and (b) the gain curve. In the quasiparticle energy approximation, the damping constant $\gamma_{aa}(\mathbf{k}) = -\text{Im}\Sigma^r_{aa}(\mathbf{k})$

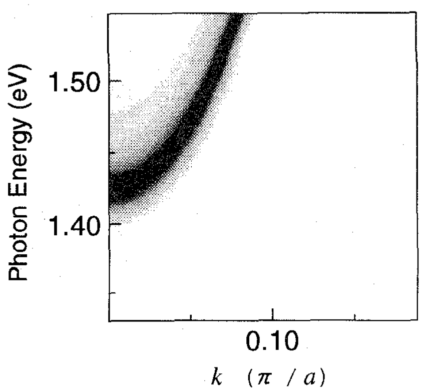

Figure 3: Energy-momentum diagram of photon spectral shape function.

depends only upon the carrier's wavenumber **k** and not upon the energy ω. As a result, the spectral shape function becomes symmetric across the band-gap as shown in Fig. 5 (a). Due to the symmetric broad spectral function, the gain curve becomes broader and decreases in the quasiparticle energy approximation. The above results mean that the quasiparticle energy approximation might underestimate the optical gain properties of semiconductor lasers.

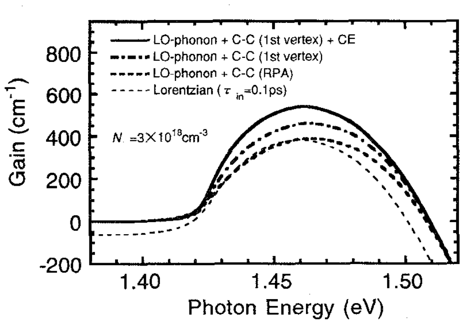

Figure 4: Optical gain spectra.

4. Conclusion

In this paper, we have studied a microscopic derivation of optical gain spectrum in semiconductor lasers. The carrier-carrier and the carrier-LO phonon interactions are considered based upon the nonequilibrium Green's function technique. It is found that the first vertex corrections in the carrier-carrier scattering and the interband Coulomb enhancement effects increase the laser gain spectra. Further, we have pointed out that the quasiparticle energy approximation might underestimate the semiconductor laser gain properties.

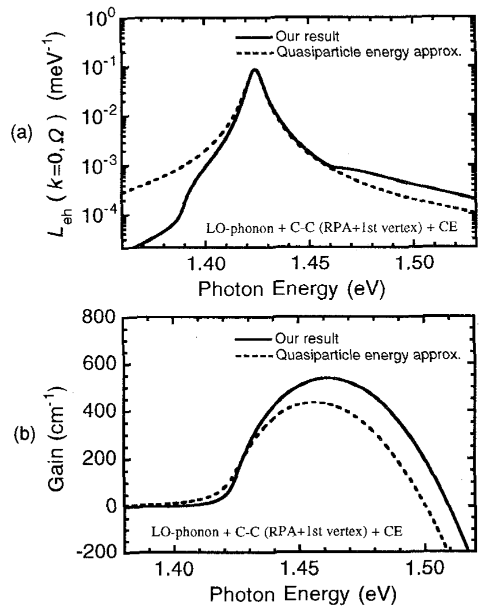

Figure 5: Comparison between our result and quasiparticle energy approximation for (a) photon spectral shape functions at k=0 and (b) optical gain spectra.

References

1. For example, M. Yamada and Y. Suematsu: J. Appl. Phys. **52** (1981) 2653; M. Asada and Y. Suematsu: IEEE J. Quantum Electron. **QE-21** (1985) 434.
2. M. Yamanishi and Y. Lee: IEEE J. Quantum Electron. **QE-23** (1987) 367.
3. M. Asada: IEEE J. Quantum Electron. **QE-25** (1989) 2019.
4. A. Tomita and A. Suzuki: IEEE J. Quantum Electron. **QE-27** (1991) 1630.
5. D. Ahn: IEEE J. Quantum Electron. **QE-32** (1996) 960.
6. S. W. Kock, *Microscopic Theory of Semiconductors: Quantum Kinetics, Confinement and Lasers* (World Scientific, Singapore, 1995).
7. H. Tsuchiya and T. Miyoshi: J. Appl. Phys. **83** (1998) 2574.
8. D. F. DuBois, *Lectures in Theoretical Physics*, edited by W. E. Brittin, A. O. Barut (Gordon and Breach, New York, 1967).
9. H. Haug and S. W. Koch, *Quantum Theory of the Optical and Electronic Properties of Semiconductors* (World Scientific, Hong Kong, 1993).